Hemocyanin of the Chiton *Acanthopleura granulata*†

Theodore T. Herskovits,* Mary G. Hamilton, and L. John Mazzella

Department of Chemistry, Fordham University, Bronx, New York 10458, and Division of Science and Mathematics, Fordham University, New York, New York 10023

Received December 16, 1985; Revised Manuscript Received February 26, 1986

ABSTRACT: The subunit structure and solution conformation of the hemocyanin of the chiton *Acanthopleura granulata* were investigated by light-scattering, ultracentrifugation, viscosity, absorbance, and circular dichroism methods. The molecular weight, determined by light scattering at pH 7.4 in the presence of 0.05 M Mg^{2+} and 0.01 M Ca^{2+}, was $(4.2 \pm 0.3) \times 10^6$, while those of dissociated subunits in the presence of 8.0 M urea (at pH 7.4) and at pH 10.7 were found to be 4.57×10^5 and 4.58×10^5, respectively. Circular dichroism and absorbance measurements at 222 and 346 nm indicate only minor changes in the conformation of the folded domains of the hemocyanin subunits in these dissociating solvents. As with the hemocyanins of the snails *Busycon canaliculatum*, *Lunatia heros*, and *Littorina littorea*, exposure to 4.0–6.0 M guanidinium chloride (GdmCl) is found to produce unfolding of the domains, resulting in much more pronounced spectral changes and a further drop in molecular weight. A M_w of 3.2×10^5 was obtained with *Acanthopleura* hemocyanin in 6.0 M GdmCl, suggesting hidden breaks in the polypeptide chains analogous to those observed with the gastropodan hemocyanins. Both urea and pH dissociation showed gradual declines in the molecular weights, consistent with a decamer–dimer–monomer scheme of subunit dissociation. The bell-shaped molecular weight profiles obtained in the pH region from 5 to 11 can be accounted for by assuming two proton-linked groups per dimer, characterized by apparent pK values of 5.5 and 9.5, and the further involvement of five to eight acidic and five to eight basic groups per monomer, having apparent pK values of 5.0 and 10.2. The urea dissociation implicates a significantly larger number of interacting groups per hemocyanin dimer and monomer and suggests hydrophobic stabilization of the subunits. A good account of the urea dissociation data, studied at pH 8.5 and a protein concentration of 0.1 $g \cdot L^{-1}$, was obtained with an apparent estimate of 30 amino acid groups (N_{app}) at the areas of contacts of each dimer forming the basic decameric assembly and an additional 100 groups per monomer forming each dimer.

The Polyplacophora or chitons represent a small class of primitive molluscs comprising about 600 living species confined exclusively to marine and shoreline habitats. As with most molluscs, the oxygen-transport protein found in the hemolymph of the chitons is a hemocyanin. Svedberg and co-workers (Svedberg et al., 1934, 1940) were the first to use the analytical ultracentrifuge to study the respiratory proteins found in the body fluids of various organisms, among them one chiton, *Tonicella marmorea*. The oxygen binding properties of several chiton hemocyanins, including those of *Katharina tunicata* and the subject of this study, *Acanthopleura granulata*, have been investigated with regard to the effects of changing both pH and temperature (Manwell, 1958, 1960; Redmond, 1962). The macromolecular structure and the corresponding states of association and dissociation have only recently gained some attention. Ryan et al. (1985) obtained a M_r of 4.2×10^6 for *K. tunicata* hemocyanin by sedimentation equilibrium and investigated the subunit structure and pH dissociation of the hemocyanin by sedimentation analyses, electron microscopy, and other physical methods. Together with the results of Ryan et al. (1985), the light-scattering and dissociation data of this paper on *A. granulata* suggest that the chiton hemocyanins share the cylindrical organization and the decameric structure proposed for the hemocyanins of the cephalopods: squids, octopuses, and nautiluses (van Holde & Miller, 1982). As a part of this study, we have examined and analyzed in some detail the effects of pH, urea, and GdmCl[1] on the dissociation of the hemocyanin decamers and have also examined the solution conformation of this hemocyanin using circular dichroism and absorbance methods.

Materials and Methods

Live chitons were obtained from the Carolina Biological Supply Co., Burlington, NC. The washed and blotted specimens were bled from incisions made at the posterior foot area or at the pallial groove region. The specimens were then placed in small funnels, and the hemolymph was allowed to drip into small beakers or flasks containing approximately 0.2 mL of a freshly prepared mixture of protease inhibitors: 0.2% trypsin inhibitor, 0.01 M EDTA, 0.01 M benzamidine, 0.02% sodium azide (Lips et al., 1982), and some PMSF crystals. Low-speed centrifugation was used to remove any particulate matter. The approximate protein concentrations determined by absorbance measurements on the clarified hemolymphs of five specimens ranged from 0.95 to 5.0%, and their pHs were between 7.39 and 7.52. Usually, 15–30 specimens were processed in each batch. The hemocyanin was purified in the cold by gel filtration chromatography on 45 × 2.5 cm columns packed with Bio-Gel A-5m in the eluent buffer:0.1 M Tris-HCl, pH 7.4, 0.05 M Mg^{2+}, and 0.01 M Ca^{2+} (Herskovits et al., 1981a,b). Only the leading fractions of the main component were used for the light-scattering studies, since most of the preparations

†Supported in part by Grant RR-0715 from the National Institutes of Health, U.S. Public Health Service.

*Address correspondence to this author at the Department of Chemistry.

[1] Abbreviations: Tris, tris(hydroxymethyl)aminomethane; GdmCl, guanidinium chloride; PMSF, phenylmethanesulfonyl fluoride; CD, circular dichroism; EDTA, ethylenediaminetetraacetic acid.

0006-2960/86/0425-3612$01.50/0

contained a second, trailing fraction of yellow material representing about 30–40% of the total protein of the hemolymph.

Protein concentrations were determined by absorbance measurements made in a Cary 14 spectrophotometer. Extinction coefficients were determined as described previously (Herskovits et al., 1985a) by using a specific refractive index increment of 0.194 $g^{-1}\cdot cm^3$ at 436 nm. For the blue hemocyanin component, the extinction coefficient $E^{1\%}_{278}$ was 15.8, and for the yellow second component it was 13.2.

Light-scattering and refractive index measurements were made at 436 nm in instruments of Brice's design (Wood Manufacturing Co.). Absolute turbidities were measured at 90° in a square cell and as a function of angle of scattered light from 35 to 145° in a cylindrical cell. The back-reflection correction of Tomimatsu and Palmer (1963) was applied to the data in the latter measurements. The protein solutions and solvents were clarified by filtration directly into the light-scattering cells (Harrington et al., 1973; Elbaum & Herskovits, 1974). Refractive index increment measurements were made on dialyzed solutions.

Circular dichroism measurements were made in a Cary 60 spectropolarimeter equipped with a CD attachment. A mean residue M_o of 120 was assumed for all the calculations in the far-ultraviolet region, together with a value of 2.5×10^4 per copper atom for the calculation of molar ellipticities in the copper-absorbing region centered at 346 nm.

Sedimentation analyses were made in a Beckman Model E analytical ultracentrifuge equipped with schlieren and photoelectric scanner-absorption optics. Usually, the sample concentrations were about 0.3–0.4%, and patterns were recorded with the schlieren optics and also scanned at 340 nm. All runs were made at room temperature at 24000 rpm. The sedimentation coefficients have been corrected to sedimentation in water at 20 °C.

Viscosity measurements were made in Cannon-Ubbelohde capillary viscometers with solvent flow times of about 250 s. Measurements were made in a constant-temperature bath at 25.0 ± 0.03 °C, usually with filtered solvent and protein solutions diluted 4–5 times directly in the reservoir of the viscometer. The protein concentrations ranged from 0.6 to 0.2%.

Results

Light-Scattering Molecular Weight of Acanthopleura granulata Hemocyanin. The light-scattering behavior of the hemocyanin component and the second component of the hemolymph, the "yellow" fraction, were investigated at the physiological pH of 7.4 (Redmond, 1962) in 0.1 M Tris buffer containing 0.05 Mg^{2+} and 0.01 M Ca^{2+} and also in the presence of the dissociating and denaturing solvents 8 M urea and 6 M GdmCl. Some of the angular-dependence and concentration-dependence data obtained with the native hemocyanin is presented in Figure 1. Similar data on the dissociated hemocyanin in urea, in GdmCl, and at high pH are shown in Figure 2. The native hemocyanin shows a very slight angular dependence, but some dissociation of the subunits apparently occurred as the protein concentration was reduced, as is shown by the increase in the values of Kc/R_θ below $c = 0.2$ g·L^{-1} (Figure 1B). The light-scattering data plotted in this figure are represented on the basis of the Zimm equation:

$$Kc/R_\theta = M_w^{-1}P(\theta)^{-1} + 2Bc \qquad (1)$$

where

$$P(\theta)^{-1} = 1 + [16\pi^2n^2/(3\lambda^2)]R_G^2 \sin^2(\theta/2) + \ldots$$

In this equation, K is the light-scattering constant, R_θ is the excess Rayleigh ratio related to the scattered light minus that of the solvent at the angle θ, M_w is the weight-average molecular weight, B is the second virial coefficient, c is the protein concentration, and $P(\theta)^{-1}$ is the reciprocal particle scattering factor related to the radius of gyration of the macromolecule, R_G; the terms defining $P(\theta)^{-1}$ have their usual meaning (Doty & Edsall, 1951).

On an average the data extrapolated to 0° (Figure 1A) gave molecular weights about 2–4% higher than the more accurate data obtained at 90° in 2.4 × 2.4 cm square cells. The con-

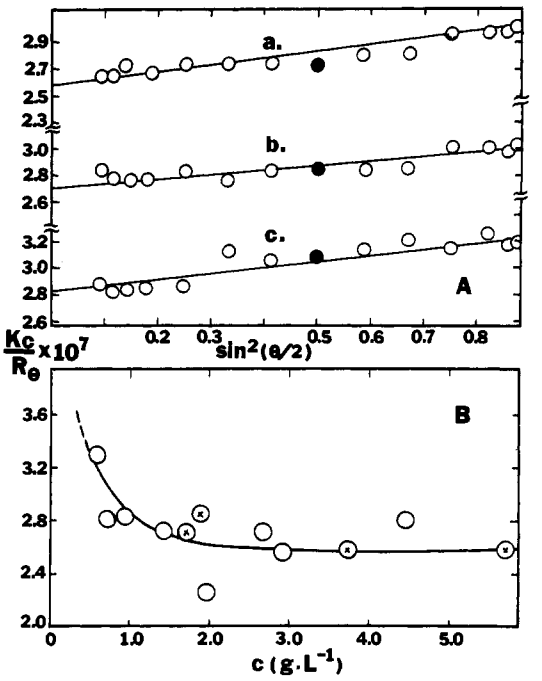

FIGURE 1: Angular and concentration dependence of the light scattering of *A. granulata* hemocyanin plotted according to eq 1–3. (A) Representative Kc/R_θ vs. $\sin^2(\theta/2)$ data obtained at hemocyanin concentrations of 3.86, 1.68, and 0.737 g·L^{-1} (curves a–c), respectively. (B) Concentration-dependence data extrapolated to zero angle, fitted according to eq 2 and 3 with $K^{10,2}_{D,app} = 5 \times 10^{-27}$ M^4, $B = 6.9 \times 10^{-10}$ L·mol·g^{-2}, and $M_{10} = (4.2 \pm 0.3) \times 10^6$. Solvent was 0.1 M Tris, pH 7.4, 0.05 M Mg^{2+}, and 0.01 M Ca^{2+}.

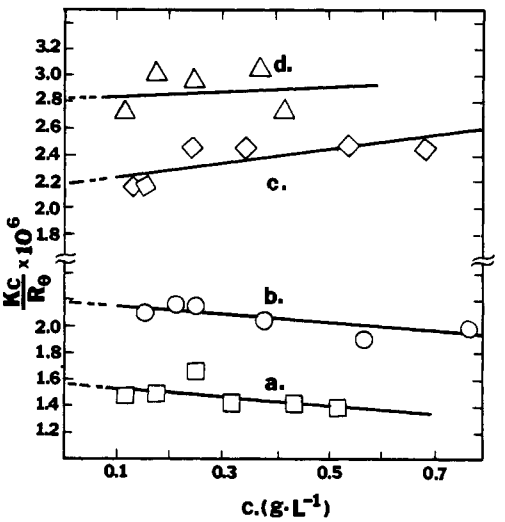

FIGURE 2: Concentration dependence of the light-scattering data of *A. granulata* hemocyanin obtained in different dissociating and denaturing solvents. (Curve a) pH 10, $\mu = 0.1$ sodium bicarbonate/NaOH; (curve b) pH 10.7, $\mu = 0.1$ bicarbonate/NaOH, 0.01 M EDTA; (curve c) 8.0 M urea, pH 7.4, 0.05 M Mg^{2+}, 0.01 M Ca^{2+}; (curve d) 6.0 M GdmCl, pH 7.4, 0.05 Mg^{2+}, 0.01 M Ca^{2+}.

Table I: Macromolecular and Spectroscopic Parameters of the Hemocyanin and Yellow Hemolymph Component of *A. granulata*

solvent	M_w	$[\eta]$ ($cm^3 \cdot g^{-1}$)	$[\theta]_{222}$ ($deg \cdot cm^2 \cdot dmol^{-1}$)	$[\theta]_{346}$ ($deg \cdot cm^2 \cdot dmol^{-1}$)	E_{278} ($dL \cdot g^{-1} \cdot cm^{-1}$)	E_{346} ($dL \cdot g^{-1} \cdot cm^{-1}$)
			Hemocyanin			
pH 7.4, μ = 0.1 Tris, 0.05 M Mg^{2+}, 0.01 M Ca^{2+}	(4.2 ± 0.3) × 10^6	7.2	−6 200 ± 200	−32 000 ± 4 000	15.8 ± 0.5	4.3 ± 0.2
pH 9.0, μ = 0.1 Tris	1.3 × 10^6		−5 700	−30 000		
pH 10, μ = 0.1 Bicarb/NaOH	6.3 × 10^5		−6 700	−32 200	14.8	3.6
pH 10.7, μ = 0.1 Bicarb/NaOH, 0.01 M EDTA	4.6 × 10^5	45	−6 200	−28 700	15.2	3.8
8.0 M urea, pH 7.4, 0.05 M Mg^{2+}, 0.01 MCa^{2+}	4.6 × 10^5	32.7	−5 300	−24 200	14.7	3.4
6.0 M GdmCl, pH 7.4, 0.05 M Mg^{2+}, 0.01 M Ca^{2+}	3.5 × 10^5	97.3	−500	−800	15.2	0.4
			Yellow Hemolymph Component			
pH 7.4, μ = 0.1 Tris, 0.05 M Mg^{2+}, 0.01 MCa^{2+}	4.30 × 10^5	8.6	−12 000		13.2	
8.0 M urea, pH 7.4, 0.05 M Mg^{2+}, 0.01 M Ca^{2+}	2.1 × 10^5	41.5	−3 760			
6.0 M GdmCl, pH 7.4, 0.05 M Mg^{2+}, 0.01 M Ca^{2+}	1.4 × 10^5	42.6	−800			

Table II: Light-Scattering Molecular Weight Data of *A. granulata* Hemocyanin

solvent	protein concn range ($g \cdot L^{-1}$)	$\partial n/\partial c$ ($g^{-1} \cdot cm^3$)	M_w	B ($L \cdot mol \cdot g^{-2}$)
pH 7.4, μ = 0.1 Tris, 0.05 M Mg^{2+}, 0.01 M Ca^{2+}	0.5–5.7	0.194	(4.2 ± 0.3) × 10^6 [a]	6.9 × 10^{-10} [a]
pH 9.0, μ = 0.1 Tris	0.2–0.9	0.184	1.28 × 10^6	3 × 10^{-9}
pH 10, μ = 0.1 bicarb/NaOH	0.1–0.5	0.191	6.34 × 10^5	−2 × 10^{-7}
pH 10.7, μ = 0.1 bicarb/NaOH, 0.01 M EDTA	0.15–0.94	0.189	4.58 × 10^5	−1 × 10^{-7}
8.0 M urea, pH 7.4, 0.05 M Mg^{2+}, 0.01 M Ca^{2+}	0.17–0.7	0.140	4.57 × 10^5	3 × 10^{-7}
6.0 M GdmCl, pH 7.4, 0.05 M Mg^{2+}, 0.01 M Ca^{2+}	0.1–0.4	0.133	3.52 × 10^5	1 × 10^{-7}

[a] Based on eq 2 and 3 with $K^{10,2}_{D,app}$ = 5 × 10^{-27} M^4 and assuming a hard-sphere B value of $4\bar{V}_2/M_{10}$ × 10^{-3} $L \cdot mol \cdot g^{-2}$.

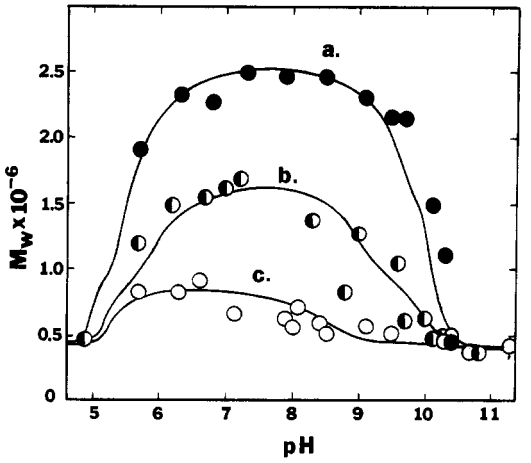

FIGURE 3: Effects of pH on dissociation of *A. granulata* hemocyanin studied in the presence of 0.01 M Mg^{2+} (a), the absence of stabilizing divalent ions (b), and the presence of 0.01 M EDTA (c). The solid lines drawn through the data points were fitted with the decamer–dimer–monomer scheme of dissociation described by eq 7–9, with the following parameters: (Curve a) $K^{10,2}_{w,app}$ = 6 × 10^{-29} M^4, $K^{2,1}_{w,app}$ = 5 × 10^{-13} M, $N_1 = N_2 = 1$, $N_3 = N_4 = 8$, $pK_1 = 5.5$, $pK_2 = 9.9$, $pK_3 = 5.0$, and $pK_4 = 10.2$; (curve b) $K^{10,2}_{w,app}$ = 1 × 10^{-27} M^4, $K^{2,1}_{w,app}$ = 5 × 10^{-11} M, $N_1 = N_2 = 1$, $N_3 = N_4 = 8$, $pK_1 = 5.5$, $pK_2 = 9.5$, $pK_3 = 5.0$, and $pK_4 = 10.2$; (curve c) $K^{10,2}_{w,app}$ = 5 × 10^{-26} M^4, $K^{2,1}_{w,app}$ = 5 × 10^{-10} M, $N_1 = N_2 = 1$, $N_3 = N_4 = 8$, $pK_1 = 5.5$, $pK_2 = 8.0$, $pK_3 = 5.0$, and $pK_4 = 9.0$. For all the calculations, M_{10} = 4.2 × 10^6 and c = 0.1 $g \cdot L^{-1}$ were employed: the 0.1 ionic strength buffers employed are described by Herskovits et al. (1985a).

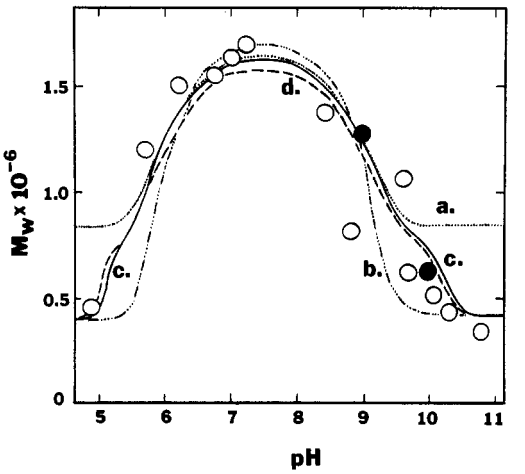

FIGURE 4: Fitting of the pH dissociation profile of *A. granulata* hemocyanin assuming one-step two-species and two-step three-species dissociation schemes described by eq 5 and 6 and 7–9, respectively. (Curve a) decamer to dimer dissociation assuming $K^{10,2}_{w,app}$ = 1 × 10^{-27} M^4, $pK_1 = 5.5$, $pK_2 = 9.5$, $N_1 = N_2 = 1$, and $m = 5$; (curve b) decamer to monomer dissociation, $K^{10,1}_{w,app}$ = 1 × 10^{-60} M^9, $pK_1 = 5.5$, $pK_2 = 9.5$, $N_1 = N_2 = 1$, and $m = 10$; (curve c) decamer–dimer–monomer scheme, $K^{10,2}_{w,app}$ = 1 × 10^{-27} M^4, $K^{2,1}_{w,app}$ = 5 × 10^{-11} M, $N_1 = N_2 = 1$, $N_3 = N_4 = 8$, and $pK_1 = 5.5$, $pK_2 = 9.5$, $pK_3 = 5.0$, and $pK_4 = 10.2$; (curve d) same model as curve c with most of the same parameters but $K^{2,1}_{w,app}$ = 5 × 10^{-10} M and $N_3 = N_4 = 5$. For all calculations, M_{10} = 4.2 × 10^6 and c = 0.1 $g \cdot L^{-1}$ values were used. M_w data: (○) 0.10 $g \cdot L^{-1}$; (●) concentration dependence data (Figure 2 and Table II).

centration-dependence data extrapolated to $\theta = 0°$ were analyzed with the equation

$$Kc/R_\theta = [M_{10}(1.0 - 0.8\alpha_2)]^{-1} + 2Bc \qquad (2)$$

and the related apparent dissociation constant

$$K^{10,2}_{D,app} = \frac{3125c^4\alpha_2^5}{M_{10}(1 - \alpha_2)} \qquad (3)$$

appropriate for the dissociation of decamers to dimers, where α_2 is the weight fraction of the protein forming dimers and M_{10} is the molecular weight of the decamer. In Figure 1B, the best fit of the data obtained for two hemocyanin preparations was obtained with $K_{D,app}$ = 5 × 10^{-27} M^4 by using the hard-sphere value ($4\bar{V}_2/M_{10}$) for the second virial coefficient, B = 6.9 × 10^{-10} $L \cdot mol \cdot g^{-2}$. The molecular weight of the *A. granulata* hemocyanin decamer, M_{10}, is found to be (4.2 ± 0.3) × 10^6, and the radius of gyration R_G is 160 ± 29 Å.

Tables I and II present summaries of molecular weight data from light-scattering measurements in various solvents for *A. granulata* hemocyanin and the yellow, second component of the hemolymph.

Effects of pH on Subunit Dissociation. The observation of Ryan et al. (1985) that the *K.* hemocyanin exhibits a gradual dissociation from the basic decamer of molluscan

hemocyanins to an equilibrium mixture of dimers and monomers prompted our detailed examination of the pH dissociation of the hemocyanin of *A. granulata*. Figures 3 and 4 present some of our results obtained at a fixed low protein concentration of 0.1 g·L^{-1} in the region from pH 5 to pH 11, in the presence and absence of stabilizing Mg^{2+} ions.

Tanford and others (Brandts, 1964; Puett, 1973) have studied the effects of pH on the denaturation equilibria of proteins and have derived expressions that account for the influence of anomalously titrating amino acid groups on the unfolding equilibria. Appling these to the dissociation behavior of subunit proteins in terms of previous formulations of protein equilibria (Herskovits & Ibanez, 1976), we have obtained equations describing the influence of pH in terms of the usual acid dissociation or ionization constants of the amino acid groups at the contact areas of the subunits (Herskovits et al., 1983). Assuming that buried groups at the contact areas of the subunits will not protonate or ionize in the pH region of interest leads to the relatively simple expression

$$K_{D,H} = K_{D,w}\prod_i [1 + (a_H/K_{D_i,H})^{\pm 1}]^{mN_H} \quad (4)$$

where $K_{D_i,H}$ represents the apparent dissociation constants of the initially buried amino groups exposed during the process of dissociation and N_H is the number of such groups per subunit. In terms of α_i or the weight fraction of protein that dissociates to m fragments or subunits, we can write

$$\frac{{\alpha_i}^m}{1-\alpha_i} = \frac{K^{j,k}_{w,app} {M_{10}}^{m-1}}{m^m c^{m-1}}[1 + a_H/10^{-pK_1}]^{mN_1}[1 + 10^{-pK_2}/a_H]^{mN_2} \quad (5)$$

and express the related weight-average molecular weight M_w as

$$M_w = M_{10}[1 - \alpha_i(m-1)/m] \quad (6)$$

Equations 5 and 6 were used to calculate curves a and b of Figure 4 for the one-step dissociation of *A. granulata* hemocyanin in the absence of Mg^{2+} by using two sets of apparent pK_i values and by taking $m = 5$ for the decamer to dimer dissociation and $m = 10$ for the decamer to monomer dissociation. It is apparent from the poor fit of the data that a more complex expression bridging the dimer to monomer transition region is required, which would also account for the fact that the ultracentrifugation data show the presence of dimeric intermediates with s rates close to 20 S. The decamer–dimer–monomer three-species scheme of subunit dissociation used in our light-scattering investigations (Herskovits et al., 1984, 1985b) seems to be adequate in terms of the α_i values and the related molecular weights given by eq 7–9. In eq 5–9,

$$\frac{{\alpha_2}^5}{1-\alpha_2} = \frac{(3.2 \times 10^{-4}){M_{10}}^4 K^{10,2}_{w,app}}{c^4(1-\alpha_3)^5}(1 + a_H/10^{-pK_1})^{5N_1}(1 + 10^{-pK_2}/a_H)^{5N_2} \quad (7)$$

$$\frac{{\alpha_3}^2}{1-\alpha_3} = \frac{K^{2,1}_{w,app} M_{10}}{20c\alpha_2}(1 + a_H/10^{-pK_3})^{2N_3}(1 + 10^{-pK_4}/a_H)^{2N_4} \quad (8)$$

$$M_w = M_{10}(1.0 - 0.8\alpha_2 - 0.1\alpha_2\alpha_3) \quad (9)$$

$K^{j,k}_{w,app}$, $K^{10,2}_{w,app}$, $K^{10,1}_{w,app}$, and $K^{2,1}_{w,app}$ represent the apparent dissociation constants of the parent decameric protein dissociating to dimers or monomers (designated by the appropriate superscripts) and the dimers dissociating to monomers; α_2 and α_3 represent the weight fraction of decamers that dissociate to dimers and the weight fraction of monomers that form from the dimeric intermediates; the four sets of pK_i and the related N_i values represent the apparent pKs and number of proton-linked amino acid groups associated with the pH dissociation of the hemocyanin assembly. The various parameters employed to fit the data of Figures 3 and 4 are listed in the legends.

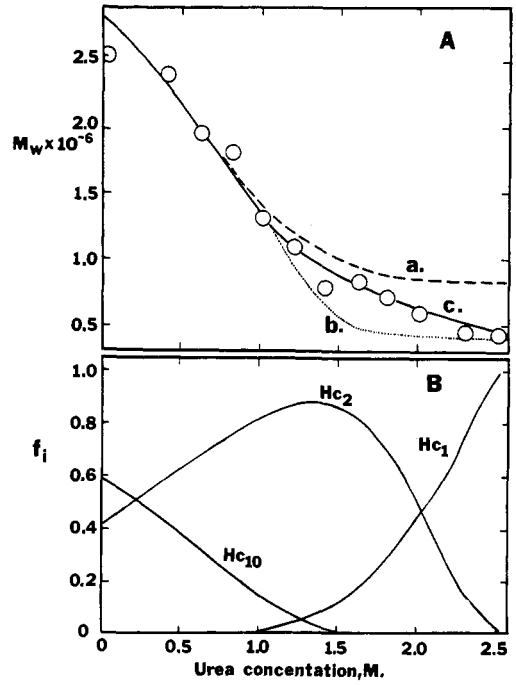

FIGURE 5: Effects of urea concentration on the light-scattering molecular weight, M_w (A), and the species distribution (B) of decameric, dimeric, and monomeric components of *A. granulata* hemocyanin at pH 8.5. (A) Analysis of the dissociation data based on eq 5–8 of Herskovits and Villanueva (1986) and eq 9–11 of the text, with the following fitting parameters: (curve a) decamer–dimer dissociation, $N^{10,2}_{app} = 30$ and $K^{10,2}_{w,app} = 5 \times 10^{-29}$ M^4; (curve b) decamer–monomer dissociation $N^{10,1}_{app} = 27$ and $K^{10,1}_{w,app} = 1 \times 10^{-53}$ M^9; (curve c) decamer–dimer–monomer dissociation; $N^{10,2}_{app} = 30$, $N^{2,1}_{app} = 100$, $K^{10,2}_{w,app} = 2 \times 10^{-29}$ M^4, and $K^{2,1}_{w,app} = 5 \times 10^{-13}$ M. For all the calculations, $M_{10} = 4.2 \times 10^6$, $K_B = 0.032$ M^{-1}, and $c = 0.1$ g·L^{-1} were used. Hemocyanin concentrations used for light scattering were 0.10 g·L^{-1}; the solvent was 0.1 M Tris, pH 8.5, 0.01 M Mg^{2+}, and 0.01 M Ca^{2+}. (B) Species distribution of decamers (Hc_{10}), dimers (Hc_2), and monomers (Hc_1) based on the molecular weight data and α_2 and α_3 estimates of the data fit (eq 10 and 11) with the fractions, f_i, of hemocyann given as $f_{10} = 1 - \alpha_2$, $f_2 = \alpha_2(1 - \alpha_3)$, and $f_1 = \alpha_2\alpha_3$ (Herskovits et al., 1984; Herskovits & Russell, 1984).

Effects of Urea and GdmCl on Subunit Dissociation. Both urea and GdmCl dissociations of *A. granulata* hemocyanin were investigated as a function of reagent concentration at the protein concentration of 0.1 g·L^{-1}, with the data obtained shown in Figures 5 and 6. We have analyzed the urea dissociation in terms of both the one- and two-step schemes from decamers to monomers or dimers and from decamers to dimers in equilibrium with monomers developed in our earlier studies (Herskovits & Russell, 1984; Herskovits et al., 1984) and used to analyze the urea dissociation data of octopus hemocyanin decamers [eq 5–12 in Herskovits & Villanueva (1986)]. Again, as with the pH dissociation, the decamer–dimer–monomer scheme described by eq 9–11 gave the best account of

$$\frac{{\alpha_2}^5}{1-\alpha_2} = \frac{(3.2 \times 10^{-4}){M_{10}}^4 K^{10,2}_{w,app}}{c^4(1-\alpha_3)^5} \exp(5N^{10,2}_{app} K_B c_D) \quad (10)$$

$$\frac{{\alpha_3}^2}{1-\alpha_3} = \frac{K^{2,1}_{w,app} M_{10}}{20c\alpha_2} \exp(2N^{2,1}_{app} K_B c_D) \quad (11)$$

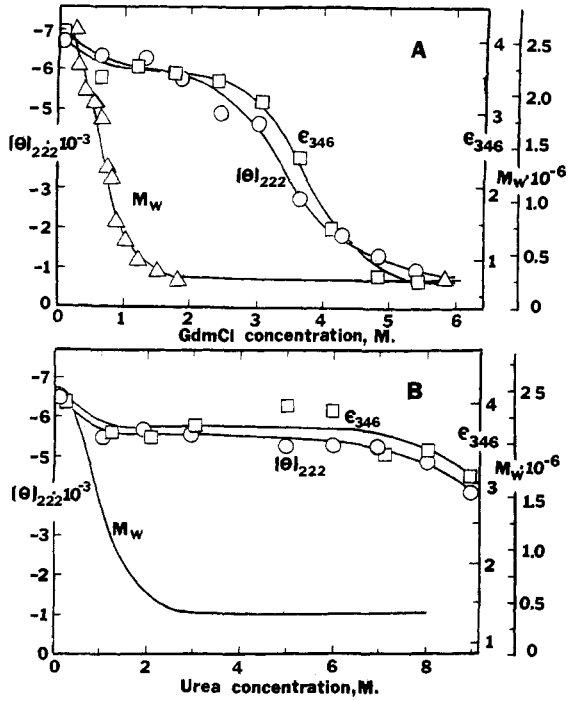

FIGURE 6: Comparison of effects of subunit dissociation and denaturation of GdmCl (A) and urea (B) on *A. granulata* hemocyanin as measured by light-scattering (M_w), circular dichroism ($[\theta]_{222}$), and copper absorbance (E_{346}). pH and ionic conditions are the same as in Figure 5 and curve a, c, and d of Figure 7.

the dissociation of *A. gralulata* hemocyanin, shown in Figure 5. In eq 10 and 11, $N_{app}^{10,2}$ and $N_{app}^{2,1}$ represent the apparent number of amino acid groups located at the contact areas of the dimers in the parent hemocyanin decamers and the number of contact groups within each monomer in the dimeric intermediates, c_D is the dissociating reagent concentration (urea) in moles per liter, and K_B is the binding or interaction constant with the average amino acid group at the contact sites of the subunits taken as 0.032 M^{-1} (Herskovits et al., 1977, 1978). The three different curves of Figure 5A represented by a–c were calculated with the two-species schemes of dissociation producing monomers and dimers as the final products and the three-species scheme with intermediate dimers dissociating to monomers, given by eq 9–11. The various parameters used to fit the data are enumerated in the legend of Figure 5.

We have also calculated the species distribution of *A. granulata* hemocyanin components present at pH 8.5 and at 0.05 M Mg^{2+} and 0.01 M Ca^{2+} at the low protein concentration of 0.01 g·L^{-1} of this study using the different sets of α_2 and α_3 values of the three-species scheme of urea dissociation. Figure 5B shows the results of our analysis represented in terms of weight fractions f_i of decamers (Hc_{10}), dimers (Hc_2), and monomers (Hc_1) produced as a result of increasing urea concentration present in the solvent.

Reversibility and Reassociation. The reassociation of *A. granulata* hemocyanin was tested by dialysis against Tris buffer of the protein dissociated by exposure to 8.0 M urea or to a high pH. Hemocyanin with the initial M_w of 4.58 × 10^5 used for the 8.0 M urea experiment (Table II) had a M_w of 1.27 × 10^6 (c = 0.21 g·L^{-1}) after dialysis against 0.1 M Tris buffer containing 0.05 M Mg^{2+} and 0.01 M Ca^{2+}. Solutions with M_w of 6.34 × 10^5 and 4.58 × 10^5 after exposure to pH 10 and pH 10.7 had M_w of 2.48 × 10^6 and 1.30 × 10^6 (c = 0.21 and 0.30 g·L^{-1}) after dialysis. These results suggest that significant, but incomplete reassociation had occurred from the fully dissociated state (in 8 M urea) and a somewhat greater degree of reassociation had occurred from the dimeric

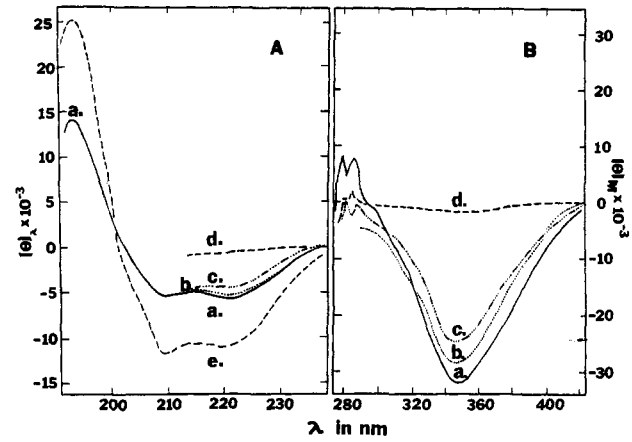

FIGURE 7: Circular dichroism spectra of *A. granulata* hemocyanin and the yellow component of the hemolymph: (curve a) *A.* hemocyanin, pH 7.4, 0.1 M Tris, 0.05 M Mg^{2+}, and 0.01 M Ca^{2+}; (curve b) pH 10.6, 0.1 ionic strength bicarbonate/OH; (curve c) 8.0 M urea, pH 7.4; (curve d) 6.0 M GdmCl, pH 7.4; (curve e) yellow hemolymph component, pH 7.4, 0.05 M Mg^{2+}, 0.01 M Ca^{2+}.

state persisting at and below pH 10. Higher M_w of (1.8–2.8) × 10^6 had been obtained in similar reassociation experiments with *Octopus bimaculoides* hemocyanin (Herskovits & Villanueva, 1986). The differences could be due to the presence of fewer proteolytic cleavages in the dissociated octopus hemocyanin chains.

Circular Dichroism and Absorbance Data at 346 nm. The effects of pH, urea, and GdmCl on the CD and absorbance spectra are shown in Figures 6 and 7. In Table I, the CD parameters at 222 and 346 nm and the absorbance data at 346 nm suggest that only marginal changes in the conformation of the folded domains occur with subunit dissociation of *A. granulata* hemocyanin. Both $[\theta]_{222}$ and E_{346} show only a slight decrease in amplitude in the urea and GdmCl concentration region where the molecular weight shows the most pronounced decline. The data shown in Figure 6 suggest that regions of the polypeptide chains connecting the copper-containing functional domains have undergone some unraveling or unfolding. The data also show that extensive changes in the folding of the subunit chains occur in GdmCl solutions above 3 M.

The mean residue ellipticity at 222 nm of the 4.3 × 10^5 dalton yellow component is −12 000 deg·cm^2·$dmol^{-1}$, whereas that of the hemocyanin is −6200 deg·cm^2·$dmol^{-1}$ (Figure 7, curves a and e). Estimates of α-helix content based on the reference parameters of Chen et al. (1972, 1974) give values of about 30 and 12% for these proteins of the hemolymph of *A. granulata.*

Sedimentation and Viscosity Data. Figure 8 presents analyses of the sedimentation behavior of *A. granulata* hemocyanin as a function of urea concentration and pH. The native hemocyanin has a sedimentation coefficient of about 60 S in the pH-stability range centering at pH 7.4 (tracings a and g). Some dissociation is suggested both by the light-scattering data of Figure 1B and by the corresponding sedimentation pattern, which shows a small amount of a slower sedimenting component. The fit of the light-scattering curve drawn through the data suggests the presence of about 7% dimers at a hemocyanin concentration of 4 g·L^{-1}. At the two ends of the pH-stability zone shown in Figure 3, we observe the presence of a significant fraction of dissociated material with s values of 21 S at pH 6.5 and 20 S at pH 9.4 (tracings f and h). The s values of this slower component shift to lower values of about 14 S at more acidic (pH 5.6) and more alkaline (pH 10.3) pHs (tracings e and i), suggesting further disso-

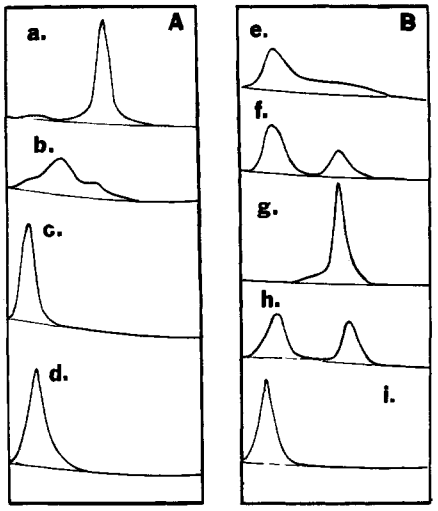

FIGURE 8: Enlarged tracings of the sedimentation patterns of *A. granulata* hemocyanin produced by 0–4.0 M urea (pH 8.5, 0.01 M Mg^{2+}, 0.01 M Ca^{2+}) (A) and pH 5.6–10.3 (0.05 M Mg^{2+}, 0.01 M Ca^{2+}) (B) Tracings: (a) 0 M urea; (b) 0.75 M urea; (c) 1.5 M urea; (d) 4.0 M urea; (e) pH 5.6; (f) pH 6.5; (g) pH 7.4; (h) pH 9.4; (i) pH 10.3. Rotor speed 24 000 rpm; protein concentration 3–4 $g \cdot L^{-1}$.

ciation of the dimers. There is a corresponding decrease in the molecular weights observed by light scattering (Table II and Figure 3). The dissociation observed in the presence of urea shows a sharp initial decline in the fraction of parent 60S material (tracing b) followed by a more gradual change in the apparent distribution of species as the parent material is depleted. In the presence of 1.5 M and higher concentrations of urea, only a single sedimenting boundary is seen (tracings c and d). The gradual decline in the apparent sedimentation coefficients from 18 S in 1.5 M urea to about 16 S in 4.0 M urea suggests a shift in equilibrium toward increased monomer (van Holde & Cohen, 1964; Siezen & van Driel, 1974).

Experimentally, the sedimentation properties of hemocyanin subunits are found to be relatively insensitive to conformational changes. Even in the random-coil form in 6.0 M GdmCl, the $s_{20,w}$ value is found to be only about half of the monomer value, or about 5 S (Herskovits et al., 1985a). The observed changes in intrinsic viscosity, $[\eta]$, seem to be much more pronounced. From initial values of about 11 $cm^3 \cdot g^{-1}$ in aqueous media and 20 $cm^3 \cdot g^{-1}$ in 8.0 M urea, the $[\eta]$ values in 6.0 M GdmCl were found to increase to 100 $cm^3 \cdot g^{-1}$ or higher (van Holde & Cohen, 1964; Salvat et al., 1979; Herskovits et al., 1985a). The changes observed for *A. granulata* hemocyanin from the pH 7.4 value of 7.2 $cm^3 \cdot g^{-1}$ to 32.7 $cm^3 \cdot g^{-1}$ in 8.0 M urea and 45 $cm^3 \cdot g^{-1}$ at pH 10.7 (Table I) suggest a significant degree of unfolding or unraveling of the connecting hinge regions of the folded domains of the subunits. Some notion of the magnitude of these changes may be gained by appropriate calculations of the intrinsic viscosity on the basis of Kirkwood's hydrodynamic theory for an extended chain of spherical beads (Kirkwood & Auer, 1951). With the inclusion of hydration δ, the intrinsic viscosity in terms of the axial ratio of length to diameter of each bead J can be expressed as

$$[\eta] = \frac{24(\bar{V}_2 + \delta V_1^\circ)J^2}{90 \ln J} \qquad (12)$$

The extended eight-domain structure of the hemocyanin monomer is characterized by $J = 8$; taking $\bar{V}_2 = 0.727$ $cm^3 \cdot g^{-1}$ and assuming 35–40% hydration (δ, in grams of water per gram of anhydrous protein), we obtain $[\eta]$ close to 9 $cm^3 \cdot g^{-1}$, which is of the correct magnitude but low. A doubling in J could be viewed as representing the unfolding of perhaps 20–30% of the domain structures and the connecting polypeptide chain regions in the monomers. This change in J triples the calculated intrinsic viscosity giving $[\eta] = 27$ $cm^3 \cdot g^{-1}$, which is in good agreement with the value obtained in 8.0 M urea. Moreover, a 20–30% change in the chain folding of the monomers is in accord with the relatively small changes observed in this solvent for the CD parameters at 222 nm from −6200 to −5300 $deg \cdot cm^2 \cdot dmol^{-1}$ and the copper absorbance at 346 nm from 4.3 to 3.4 $dL \cdot g^{-1} \cdot cm^{-1}$ (Table I).

Discussion

The observed weight-average M_w of $(4.2 \pm 0.3) \times 10^6$ obtained by light scattering for *A. granulata* hemocyanin is identical with the molecular weight obtained by sedimentation equilibrium for the hemocyanin of the chiton *K. tunicata* (Ryan et al., 1985). The light-scattering molecular weights of the dissociated subunits of *A. granulata* hemocyanin in 8 M urea and at pH 10.7, 4.57×10^5 and 4.58×10^5 (Table II), are within 10% of the expected value assuming 10 subunits for each decameric assembly as observed for nautilus and octopus hemocyanins (Bonaventura et al., 1981; Miller & van Holde, 1982; Herskovits & Villaneuva, 1986). The circular dichroism spectra in the peptide-absorbing ultraviolet region and in the copper-absorbing region at 346 nm remain largely unaltered in these two solvents (Figure 7 and Table I), suggesting that the folded segments of the hemocyanin subunits comprising the copper-containing functional domains escape denaturation. Complete denaturation and unfolding of the polypeptide chains is observed, however, in 5–6 M GdmCl solutions, as is shown by changes in both the CD spectra and the absorbance at 346 nm (Figures 6 and 7). Unfolding of the subunits in 6 M GdmCl results also in the further decrease in the M_w to 3.52×10^5 (Table II), which is less than one-tenth of the molecular mass of the parent hemocyanin. Similar changes noted in the molecular weights of other molluscan hemocyanins (Brouwer & Kuiper, 1973; Wood & Peacocke, 1973; Herskovits et al., 1985a,b) have been attributed to the exposure of hidden breaks in some of the chain segments of the unfolded subunits.

The hemolymphs of the limited number of chitons that have been investigated so far contain a relatively large fraction of yellow material representing about 30–60% of the total absorption at 280 nm. This has been observed in the hemolymphs of the chitons *K. tunicata* and *Chiton tuberculatus* (Redmond, 1962; Ryan et al., 1985) as well as for the hemolymphs of *A. granulata*, *Stenoplax conspicua*, *Mopalia muscosa*, and *Cryptochiton stelleri* in our laboratory. The light-scattering molecular weight of the yellow component of the hemolymph of *A. granulata* was found to be 4.3×10^5 (Table I), which is close to one-tenth of the molecular weight of the native hemocyanin. The sedimentation pattern showed a broad 20S boundary. It had an intrinsic viscosity of 8.6 $cm^3 \cdot g^{-1}$ and a mean residue ellipticity of −12 000 $deg \cdot cm^2 \cdot dmol^{-1}$ at 222 nm. The physiochemical data obtained on this material suggest that it has a more compact and more helical conformation than the hemocyanin monomer. The mean residue ellipticity indicates the presence of about 30–35% α-helical folding for this component relative to 10–12% α-helix for the hemocyanin component of the hemolymph, with a mean residue ellipticity of −6200 $deg \cdot cm^2 \cdot dmol^{-1}$ (Figure 7). These observations tend to rule out the possibility that the yellow component of the hemolymph is some precursor or a modified form of the hemocyanin monomer that is incapable of forming decamers under physiological conditions. However, the presence of such a large fraction of high molecular weight protein circulating

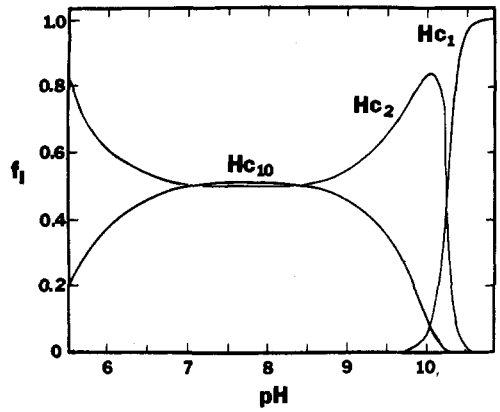

FIGURE 9: Effects of pH on species distribution of *A. granulata* hemocyanin based on the molecular weight data of Figure 3, obtained in the presence of 0.01 M Mg^{2+} and a protein concentration of 0.10 g·L^{-1} (curve a). The fractions of species, f_i, present were calculated from the α_2 and α_3 values generated by eq 7 and 8 as described in the legend of Figure 5B, with the $K^{j,k}_{w,app}$, and pK_i parameters of Figure 3, curve a.

in the hemolymph poses several interesting questions regarding its origin and function, which will have to be explored further.

The 4.2 × 10^6 dalton decameric assembly of *A. ganulata* hemocyanin is characterized by a sedimentation coefficient of 60 S. However, even at physiological pH and ionic conditions, i.e., in the presence of 0.01–0.05 M Mg^{2+} and 0.01 M Ca^{2+}, the ultracentrifugal patterns show some dissociation to dimeric components with sedimentation coefficients close to 20 S (Figure 8, tracings a and g). The dissociation is more clearly seen at acidic pHs of 6.5 and below and at alkaline pHs of 9.4 and above (Figure 8, tracings f and h). The shift in *s* values from 21 S to about 16 and 14 S noted with both urea and pH dissociation probably signify shifts in equilibria toward the fully dissociated monomeric subunits[2] with measured molecular masses of 4.58 × 10^5 and 4.57 × 10^5 daltons at pH 10.7 and in 8.0 M urea, respectively (Table II).

The more detailed quantitative examination of the bell-shaped molecular weight profile of the pH stability of *A. granulata* hemocyanin shown in Figures 3 and 4 requires the presence of a dimeric intermediate in the dissociation scheme of decamer to dimer to monomer. Moreover, the triggering mechanism for both acid and alkaline dissociation requires only a few key protonating or ionizing groups to destabilize the decameric assembly. Thus, the fit of the initial decline in molecular weight data requires only two groups with p*K* values of 5.5 and 9.5–9.9 per monomer or dimer, respectively, to generate the observed bell-shaped M_w vs. pH curve. Further refinement of the data fit presented in Figure 4 suggests that the dissociation of the dimeric intermediates involves the titration of five to eight acidic and five to eight basic groups per monomer with apparent p*K* values in the range of 5 and 10. At the acid end of the observed molecular weight transition usually glutamic or aspartic acid side chains and histidine residues are protonated, while at the alkaline end the normal range of ionization of lysine and tyrosine residues is from about 9.5 to 10.5 (Tanford, 1961). The p*K* values employed to fit the molecular weight data clearly implicate the participation of such groups in the proton-linked association–dissociation reaction of *A. granulata* hemocyanin. In sharp contrast to the relatively few ionic groups involved in the pH dissociation, the urea dissociation formulated with the same three species of macromolecular components interacting with the dissociating solvent required about 30 amino acid groups per dimer (N_{app}) and about 100 groups per monomer to produce the observed molecular weight decline studied as a function of urea concentration (Figure 5).

The species distribution plots based on the pH and urea dissociation transitions shown in Figure 5B and 9 are equally informative. With the chiton hemocyanin dissociation, we see relatively little overlap in the decamer and monomer species and a significant accumulation of dimeric intermediates before the monomers predominate. This would help to explain the relatively broad dissociation profiles as well as the high pH required for the dissociation of the dimeric components of chiton hemocyanins. With increasing pH, Ryan et al. (1985) observed a gradual decrease in sedimentation coefficient of the 20S component of *K. tunicata* hemocyanin.

The relatively large apparent number of subunit contacts (N_{app}) obtained with urea as the dissociating agent is important in regard to both the nature of the two types of subunit contacts that stabilize the basic decameric assembly of the molluscan hemocyanins and the forces that hold the subunits together in aqueous solution. The larger N_{app} values of the monomers, about 100 amino acid groups, together with the 10–16 acidic and basic groups that ionize at both ends of the pH dissociation curve would help to explain the greater stability of the dimers and the high pH and high urea concentrations required for their complete dissociation. The tight organization of the dimers and their intertwined character, suggested earlier as an explanation for the larger N_{app} values of the monomers relative to dimers within each decamer (Herskovits & Villanueva, 1986), would also serve to explain the exceptional stability of the molluscan hemocyanins toward urea and GdmCl denaturation (Figure 6). Work in progress with *A. granulata* hemocyanin as well as three other chiton hemocyanins indicate that the predominantly hydrophobic character of the side-to-side contacts of the subunits within each decamer is shared with the other gastropod and cephalopod hemocyanins of the molluscan phylum.

[2] For the hemocyanin of the squid *Loligo pealei*, van Holde and Cohen (1964) attributed a decrease in the sedimentation coefficient from 19S to 11S as a shift in the composition of a rapidly equilibrating monomer–dimer mixture toward monomers of molecular mass of 3.85 × 10^5 daltons.

REFERENCES

Bonaventura, C., Bonaventura, J., Miller, K. I., & Van Holde, K. E. (1981) *Arch. Biochem. Biophys. 211*, 589–598.

Brands, J. F. (1964) *J. Am. Chem. Soc. 86*, 4302–4314.

Brouwer, M. E., & Kuiper, H. A. (1973) *Eur. J. Biochem. 35*, 428–435.

Chen, Y. H., Yang, Y. T., & Martinez, H. M. (1972) *Biochemistry 11*, 4120–4131.

Chen, Y. H., Yang, Y. T., & Chau, K. H. (1974) *Biochemistry 13*, 3350–3359.

Doty, P., & Edsall, J. T. (1951) *Adv. Protein Chem. 6*, 35–121.

Elbaum, D., & Herskovits, T. T. (1974) *Biochemistry 13*, 1268–1278.

Harrington, J. P., Pandelfelli, E. R., & Herskovits, T. T. (1973) *Biochim. Biophys. Acta 326*, 61–73.

Herskovits, T. T., & Ibanez, V. S. (1976) *Biochemistry 15*, 5715–5721.

Herskovits, T. T., & Russell, M. W. (1984) *Biochemistry 23*, 2812–2819.

Herskovits, T. T., & Villanueva, G. B. (1986) *Biochemistry 25*, 931–939.

Herskovits, T. T., Cavanagh, S. M., & San George, R. C. (1977) *Biochemistry 16*, 5795–5801.

Herskovits, T. T., San George, R. C., & Cavanagh, S. M. (1978) *J. Colloid Interface Sci. 63*, 226–234.

Herskovits, T. T., Erhunmwunsee, L. J., San George, R. C., & Herp, A. (1981a) *Biochim. Biophys. Acta 667*, 44–58.
Herskovits, T. T., San George, R. C., & Erhunmwunsee, L. J. (1981b) *Biochemistry 20*, 2580–2587.
Herskovits, T. T., Jacobs, R., & Nag, K. (1983) *Biochim. Biophys. Acta 742*, 142–154.
Herskovits, T. T., Russell, M. W., & Carberry, S. E. (1984) *Biochemistry 23*, 1873–1881.
Herskovits, T. T., Carberry, S. E., & Villanueva, G. B. (1985a) *Biochim. Biophys. Acta 828*, 278–289.
Herskovits, T. T., Mazzella, L. J., & Villanueva, G. B. (1985b) *Biochemistry 24*, 3862–3870.
Kirkwood, J. G., & Auer, P. (1951) *J. Chem. Phys. 19*, 281–283.
Lips, D., Gielens, C., Preaux, G., & Lontie, R. (1982) *Arch. Int. Physiol. Biochim. 90*, B128.
Manwell, C. (1958) *J. Cell. Comp. Physiol. 52*, 341–352.
Manwell, C. (1960) *Arch. Biochem. Biophys. 89*, 194–201.
Miller, K. I., & van Holde, K. E. (1982) *Comp. Biochem. Physiol., B: Comp. Biochem. 73B*, 1013–1018.
Puett, D. (1973) *J. Biol. Chem. 248*, 4623–4633.
Redmond, J. R. (1962) *Physiol. Zool. 35*, 304–313.
Ryan, M., Terwilliger, N. B., Terwilliger, R. C., & Schabtach, E. (1985) *Comp. Biochem. Physiol., B: Comp. Biochem. 80B*, 647–656.
Salvato, B., Ghiretti-Magaldi, A., & Ghiretti, F. (1979) *Biochemistry 18*, 2731–2736.
Siezen, R. J., & van Driel, R. (1974) *J. Mol. Biol. 90*, 91–102.
Siezen, R. J., & Van Bruggen, E. F. J. (1974) *J. Mol. Biol. 90*, 77–89.
Svedberg, T., & Hedenius, A. (1934) *Biol. Bull. (Woods Hole, Mass.) 66*, 191–223.
Svedberg, T., & Pedersen, K. O. (1940) *The Ultracentrifuge*, Oxford University Press, Oxford, England.
Tanford, C. (1961) *Physical Chemistry of Macromolecules*, Chapters 4, 6, and 8, Wiley, New York.
Tanford, C. (1970) *Adv. Protein Chem. 24*, 1–95.
Tomimatsu, Y., & Palmer, K. J. (1963) *J. Phys. Chem. 67*, 1720–1722.
van Holde, K. E., & Cohen, L. B. (1964) *Biochemistry 3*, 1803–1808.
van Holde, K. E., & Miller, K. I. (1982) *Q. Rev. Biophys. 15*, 1–129.
Wood, E. G., & Peacocke, A. R. (1973) *Eur. J. Biochem. 35*, 410–420.

Internal Cavities and Buried Waters in Globular Proteins†

Alexander A. Rashin,‡ Michael Iofin, and Barry Honig*
Department of Biochemistry and Molecular Biophysics, Columbia University, New York, New York 10032
Received August 30, 1985; Revised Manuscript Received January 27, 1986

ABSTRACT: A fast algorithm that detects internal cavities in proteins and predicts the positions of buried water molecules is described. The cavities are characterized in terms of volume, surface area, polarity, and the presence of bound waters. The algorithm is applied to 12 proteins whose structures are known to high resolution and successfully predicts the locations of over 80% of internal water molecules. Most proteins are found to have a number of internal cavities ranging in volume from 10 to 180 Å^3. Some of these cavities contain water and some do not, with the probability of containing a buried water increasing with cavity size. However, many large cavities are found to be empty (i.e., they do not contain a crystallographically determined water). For multidomain proteins over half of the total cavity volume is at the interdomain interface. Possible implications for the energetics of cavity formation and for the functional role of internal cavities are discussed.

It has been shown in a number of studies that the packing density in globular proteins is similar to that found in crystals of small organic molecules (Richards, 1974; Finney, 1975; Schultz & Schirmer, 1979). Since a random sequence of amino acids would not be expected to generate a tightly packed structure, close packing has been suggested as a criterion to be used in protein folding studies (Schulz & Schirmer, 1979; Rashin, 1980). On the other hand, internal cavities large enough to accommodate xenon atoms have been found to exist in proteins (Schoenborn, 1969; Richards, 1974; Tilton et al., 1984). Internal cavities have been associated with conformational flexibility (Lumry & Rosenberg, 1975), the mechanism of hydrogen exchange (Richards, 1979), and, more recently, the existence of multiple side chain conformations of a single protein (Smith et al., 1986). Despite their apparent importance there is little information available as to the detailed properties of cavities in proteins.

It would be of interest, for example, to determine the size of cavities that are permissible in a particular structure and to have a means of determining whether a particular cavity is likely to be filled with water molecules. These questions are likely to assume considerable importance in prediction algorithms for protein conformation. The type of problem that can be encountered in model building has been illuminated by the study of Novotny et al. (1984), who succeeded in generating apparently reasonable but nevertheless incorrectly folded structure for two proteins (for example, by using the C^α coordinates of hemerythrin, which is α-helical, to generate a hemerythrin-like structure with a sequence of an immunoglobulin domain, which is known to be primarily β-sheet). An analysis of cavity size in the incorrectly folded structures might, for example, show them to be unrealistic and thus provide criteria for their evaluation.

† This work has been supported by grants from the NIH (GM30518) and NSF (PCM82-07145 and DMB85-03484).
‡ Present address: Department of Physiology and Biophysics, Mount Sinai School of Medicine, New York, New York 10029.

0006-2960/86/0425-3619$01.50/0